Joint International Topical Meeting on Mathematics & Computation and Supercomputing in Nuclear Applications (M&C + SNA 2007)
Monterey, California, April 15-19, 2007, on CD-ROM, American Nuclear Society, LaGrange Park, IL (2007)

AN EMBEDDED SEMI-ANALYTICAL BENCHMARK VIA ITERATIVE INTERPOLATION FOR NEUTRON TRANSPORT METHODS VERIFICATION

B. D. Ganapol
Department of Aerospace and Mechanical Engineering
University of Arizona
Ganapol@cowboy.ame.arizona

K.T.Clarno and Seth Johnson
Nuclear Science and Technology Division, ORNL
clarnokt@ornl.gov

Cassiano de Oliveira and Steven Hamilton
Nuclear and Radiological Engineering and Medical Physics
Georgia Institute of Technology
c.oliveira@gatech.edu

ABSTRACT

A new multidimensional semi-analytical benchmark capability is developed. The key feature in the solution is the point kernel formulation. The 3D nature of the source is inherited in the flux making this a true multidimensional test. In addition, an efficient numerical scheme, called iterative interpolation, is used to evaluate the required point kernel solution and maintain benchmark accuracy. The **EVENT** finite element transport algorithm is compared to the point source solution as the first step of embedding the benchmark directly with the **EVENT** code. Additional code comparisons will be presented

KEYWORDS: Verification, Analytical solution, Point source, Fourier transform, **EVENT** code

1. INTRODUCTION

Increased computational speed and storage have changed the way we think of and apply semi-analytical neutron transport benchmarks. In the past, a semi-analytical benchmark was simply a highly accurate evaluation of a tractable analytical solution to the transport equation. The evaluation would routinely involve numerical methods whose numerical error could be tightly controlled--hence, the ability to generate a highly accurate standard to which more approximate methods could be compared. There are several obvious issues concerning semi-analytical benchmarks that have seriously limited their application however. In particular, until recently, semi-analytical benchmarks could only be applied to the most basic transport problems. While this is a significant limitation for realistic transport scenarios, it does not diminish their value as one of several verification tools since even the most sophisticated transport code must adequately solve the most fundamental problem. This requirement often escapes transport methods developers who are reluctant to submit their code to benchmark testing and thereby possibly compromising code performance. Thus, even with this limitation, comparisons to semi-

analytical benchmarks are essential for proper transport methods development. This presentation, however, is concerned with generating and incorporating more comprehensive benchmarks into existing code development efforts.

One of the fundamental transport methods that was developed early on, is the point kernel method [1]. At the heart of the method is the most basic point kernel which when integrated over the appropriate source strength distribution provides an estimate of the flux of particles arriving at a particular point of interest. This simple concept is probably one of the most primitive, but at the same time can provide much needed flux approximations required for shield design in relatively complicated geometries in a timely manner. In this presentation, we reconsider the point kernel technique but now include scattering explicitly. Here, we are limited to an infinite medium, but the flux distribution can be multidimensional—inheriting its dimensionality from the source. In this way, a true 3D benchmark is realized, albeit in an infinite medium. We begin with a brief description of how the one-group point source kernel is derived followed by its numerical implementation. The implementation features several new concepts that have emerged as a result of the improved computational environment. In particular, a new Fourier transform inversion will be introduced along with an iterative interpolation to speedup the calculation and allow consideration of more comprehensive sources and error control. In addition, a demonstration of an embedded benchmark appropriate for the **EVENT** finite element code [2] will be included.

2. FLUX FROM A POINT SOURCE: THEORY

The theory begins with the solution of the one-group transport equation in an anisotropically scattering plane infinite medium with isotropic source emission

$$\left[\mu\frac{\partial}{\partial x}+1\right]\Psi(x,\mu)=\frac{c}{2}\sum_{l=0}^{L}\omega_l P_l(\mu)\Psi_l(x)+\frac{\delta(x)}{2}. \tag{1}$$

The Legendre moments $\Psi_l(x)$ are defined as

$$\Psi_l(x)\equiv\int_{-1}^{1}d\mu P_l(\mu)\Psi(x,\mu)$$

and the particle flux distribution is required to remain finite i.e., $\lim_{|x|\to\infty}\Psi(x,\mu)<\infty$. Note that any scattering order *L* is allowed. By application of the Fourier transform and the subsequent generation of two separate equations for the scattering moments, the following explicit Fourier transform inversion is found [3]:

$$\Psi_0(x)\equiv\frac{1}{2\pi}\int_{-\infty}^{\infty}dk\ e^{ikx}\left[\frac{\tilde{g}_L(z)}{\Lambda_L(z)}\right]. \tag{2}$$

with $z \equiv \frac{1}{ik}$ and

$$\Lambda_L(z) = (L+1)\left[g_{L+1}(z) Q_L(z) - g_L(z) Q_{L+1}(z) \right]$$
$$\tilde{g}_L(z) = (L+1)\left[\rho_{L+1}(z) Q_L(z) - \rho_L(z) Q_{L+1}(z) \right].$$

$g_l(z)$ and $\rho_l(z)$ satisfy a well-known recurrence relation and are called Chandrasekhar polynomials of the first and second kinds respectively [4]. $Q_l(z)$ is the Legendre function of the second kind.

The scalar flux from a point source is simply obtained from the plane/point transformation [5]

$$\Phi_{pt}(r) = -\frac{1}{2\pi r}\frac{d\Psi(r)}{dr} \tag{3}$$

which gives from Eq(2)

$$\Phi_{pt}(r) \equiv \frac{1}{2\pi}\int_{-\infty}^{\infty} dk\, e^{ikr}\left[\frac{\tilde{g}_L(z)}{z\Lambda_L(z)}\right]. \tag{4}$$

The task is now to evaluate the Fourier transform inversion integral numerically.

3. NUMERICAL IMPLEMENTATION OF A 3D BENCHMARK WITH ITERATIVE INTERPOLATION

3.1 Numerical Fourier transform inversion

To evaluate the Fourier inversion integral, a novel strategy, borrowed from the numerical evaluation of Laplace transform inversions called Talbot's method [6], adopted.

Consider the analytical continuation of the integrand to the contour shown in Fig. 1. The original inversion contour, along the entire real axis, can be replaced by contour ABCDE which surrounds the cut $[i,\infty]$. The chosen contour is indicated, where *u* is on the real axis. $g(u)$ is specified to approach infinity as *u* approaches either $\pm a$. It can then be shown that the contour integral becomes

$$\Phi_{pt}(r) \equiv \frac{1}{\pi}\int_0^a du\, e^{-ug(u)r}\, Re\left\{\frac{dz}{du}\left[\frac{\tilde{g}_L(z(u))}{z(u)\Lambda_L(z(u))}\right] e^{iur}\right\} \tag{5}$$

which is now an integral over a finite interval $[-a,a]$ making its evaluation more straightforward than the original integration. This formulation can greatly reduce the number of function evaluations even though the integrand may still oscillate.

3.2 Iterative interpolation (i^2)

Consider a 2D plane source as shown in Fig. 2. The scalar flux at a detector (also indicated) is to be found. Assuming a uniform source strength and by considering the source to be composed of infinitesimal point sources, the flux at the detector is

$$\Phi(r,\theta,z) = S_0 \int_{A_s} d\vec{r}' \Phi_{pt}\left(\left|\vec{r}-\vec{r}'\right|\right) \tag{6}$$

where $\vec{r}-\vec{r}'$ is the vector between any point on the source and the detector.

$$z = u\left(1+g(u)i\right), \quad -a \le u \le a$$

$$g(u) = \mathrm{Tan}\left(\frac{\pi u}{2a}\right) \to \infty, \quad u = \pm a$$

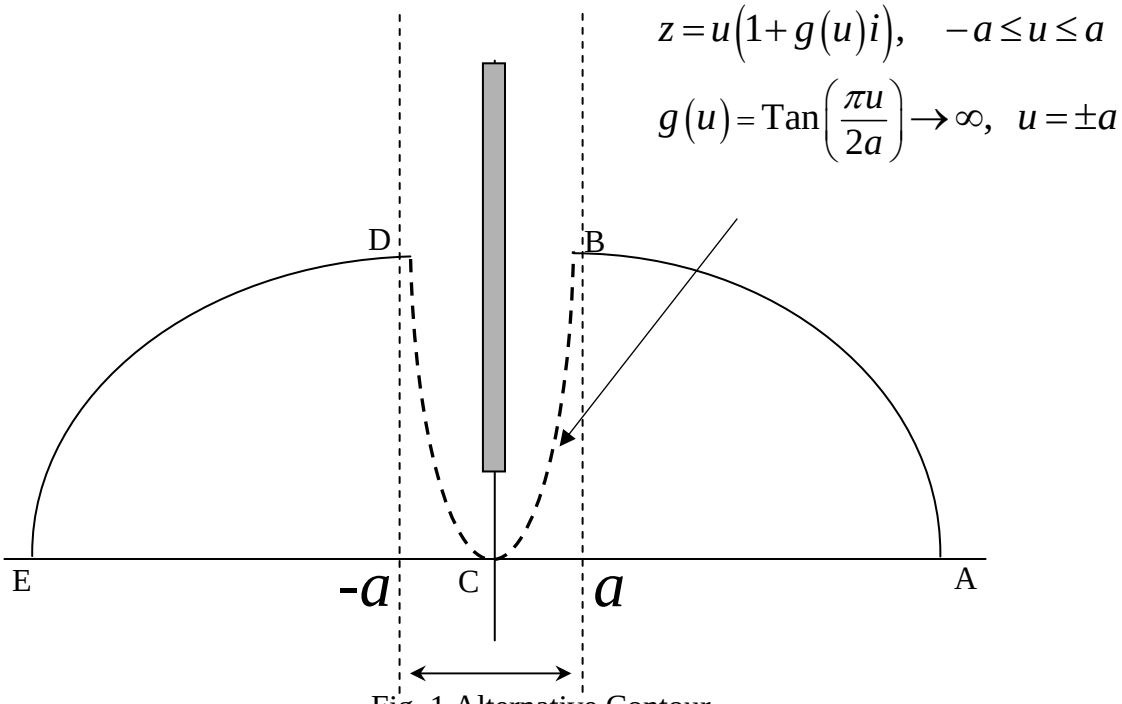

Fig. 1 Alternative Contour

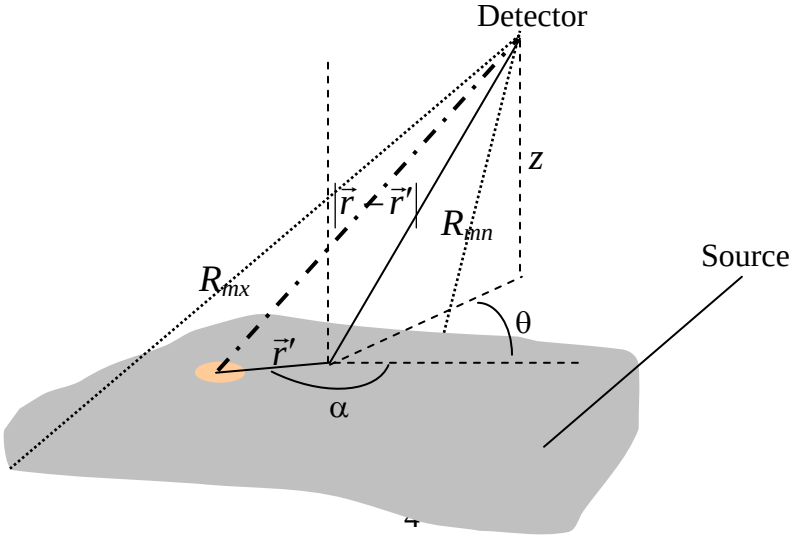

Fig. 2 General plane source configuration

To evaluate this integral, we first choose a 2D quadrature scheme to approximate the integral in Eq(6)

$$\Phi\left(r,\theta,z\right)\cong S_0\sum_{m'}\omega_{m'}\Phi_{pt}\left(\left|\vec{r}-\vec{r}_{m'}\right|\right). \tag{7}$$

In general, the evaluation of Eq(7) would require many point source flux determinations to arrive at four-place benchmark accuracy. In order to reduce the calculational effort, an iterative interpolation (i^2) has been devised. The initial step is to determine the maximum and minimum distances, R_{mx} and R_{mn}, to the detector from any point on the source. Next, the flux from the point source, as described above, is numerically evaluated at N equally spaced "base points" between these values. A rational interpolation then gives $\Phi_{pt}\left(\left|\vec{r}-\vec{r}_{m'}\right|\right)$ for the quadrature abcissae $\vec{r}_{m'}$. Finally, N is set to N+2 and the desired flux is recalculated. The procedure is continued until convergence in the number of base points N at specified edit points is achieved.

4. DEMONSTRATION: DISK SOURCE BENCHMARK SERIES (DSBS)

4.1. Double integration over the disk source without i^2

For this benchmark series (DSBS), either full or partial disk sources as shown in Fig. 3 will be implemented. The challenge is to achieve the highest possible accuracy for minimal integration effort over the entire source. For this case, Eq(6) becomes

$$\phi\left(\rho,\theta,z\right)=S_0\int_0^R dr'r'\int_{-\theta_0/2}^{\theta_0/2}d\theta'\phi_{pt}\left[\sqrt{r'^2+\rho^2+z^2-2r'\rho\cos\left(\theta'-\theta\right)}\right] \tag{8}$$

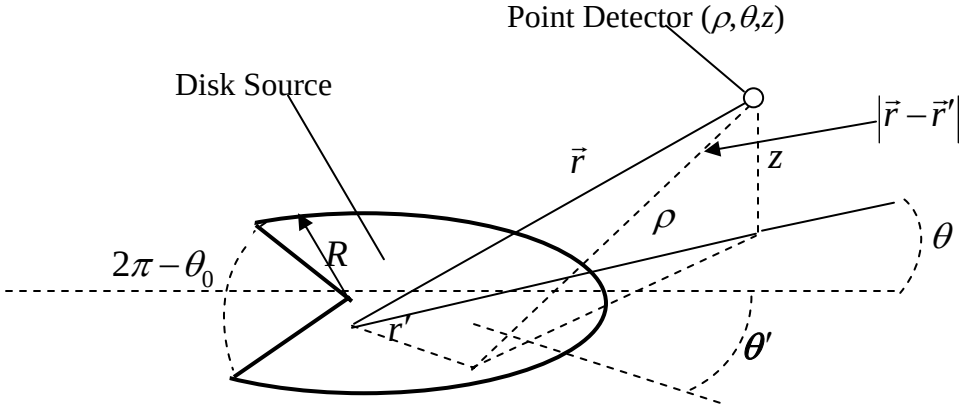

Fig. 3 DSBS geometry

for a disk wedge of angle θ_0 and radius *R*. Uniform source strength S_0 is assumed. Numerically, the integrals in Eq(8) have been found to be best accommodated through the trusted shifted Gauss-Legendre quadrature without any change of variable. Both quadratures are performed for the same order *Lm*.

As a demonstration and to assess the challenge of the disk source series, a 15 deg wedge disk source of radius 0.5*mfp* in an anisotropically scattering infinite medium (*c* = 0.9; Henyey-Greenstein, *g* = 0.9, *L*=12) is considered. The flux is interrogated on a plane above and parallel to the source. Fig. 4a shows the detector response on a plane 0.1 *mfp* above the source. The scalar flux at a total of 10^4 points was obtained at a relative error of 10^{-4} without regard to source symmetry and required 47s on a 2.8 GHz processor. Approximately, $1.4\text{x}10^6$ point source flux determinations were performed. The direct determination of the point fluxes becomes prohibitive when an additional iteration on quadrature order for the integrals over the distributed source is envisioned to guarantee benchmark accuracy. Thus, i^2 will definitely be necessary.

4.2 Double integration over the disk source with i^2

The maximum and minimum distances from any point on the source to any point on the detector plane are

$$r_{\min} = z$$
$$r_{\max} = \sqrt{\left(R + L/2\right)^2 + z^2}.$$

Since

$$r_{\min} \le \left|\vec{r} - \vec{r}'\right| = \sqrt{r'^2 + \rho^2 + z^2 - 2r'\rho\cos\left(\theta' - \theta\right)} \le r_{\max},$$

all points in the integration specified by Eq(8) can be obtained from the interpolation between the N_{int} "base points" of Fig. 4b.

Figure 4c shows the comparison of the flux on the detector plane for a 10-point interpolation and the flux without interpolation for *Lm* = 12. The maximum relative error is $1.8\text{x}10^{-5}$, which is within the desired relative error (10^{-4}) and is an excellent indication of the effectiveness of the interpolation. The time of computation is reduced by a factor of 3.6, which is certainly significant when extension to a 3D source with multiple quadrature is considered.

To this point, the interpolation demonstration has been for a fixed quadrature order only (*Lm* = 12); but as indicated above, iteration in quadrature order will be required for a legitimate benchmark. With i^2, such iteration can now be included for a reasonable computational effort. Table 1 shows the maximum flux error between quadrature orders to convergence for a 10-point interpolation for the above case. Convergence occurs at *Lm* = 16. The computational effort is less than 20s for the 10-point interpolation, less than 8s for the 5-point interpolation compared to 375s for the full calculation.

5. BENCHMARK APPLICATION: THE EVENT TRANSPORT CODE

In this section, we present the details of the **EVENT** code solution comparison with the basic point source benchmark problem. **EVENT** is a general purpose, unstructured grid code based on a multigroup anisotropic finite element-spherical harmonics framework. The solution of the benchmark problem was attempted on a sphere of 20*mfp* radius with c = 0.9 and a white boundary condition on the surface. A spherical isotropic source of 0.1*mfp* radius and unit strength was used to simulate the point source. The problem was solved in both 1D spherical geometry and 3D geometry. In the latter, only a reflected octant was considered.

Table 2 shows the results of the 2 calculations for a given spatial resolution and 3 angular approximations. The results show that the **EVENT** 3D solutions are reasonably accurate, but the mesh still needs further refinement.

This demonstration is the first step in embedding a point source benchmark directly into the **EVENT** code at a callable diagnostic level. The diagnostic can be actuated by performing a significant number of code modifications or porting the code to another platform. In this way, the semi-analytical benchmark will provide constant vigilance of **EVENT** protecting it from intentional or unintentional abuse.

REFERENCES

1. R.V. Meghreblian and D.K. Holmes, *Reactor Analysis*, McGraw-Hill, NY, 1960.
2. C. R. E. DE Oliveira and A. J. H. Goddard, *Proceedings of the OECD International Seminar on 3D deterministic radiation transport codes*, Paris, 1-2 December 1996, 81 (1996).
3. B.D. Ganapol, **TIEL**: *Analytical Benchmark for Neutron Transport in Infinite Media* (*Source Series* 1), Issued by the ANS/Joint Benchmark Committee, 2007.
4. E. Inonu, *Jour. Math. Phys*., V11, 568 (1973).
5. K. Case and P. Zweifel, *Linear Transport Theory*, Addison Wesley, MA, (1967).
6. A. Talbot, "The accurate numerical inversion of Laplace transforms", *J. Inst. Math. Appl.* 23 (1979).

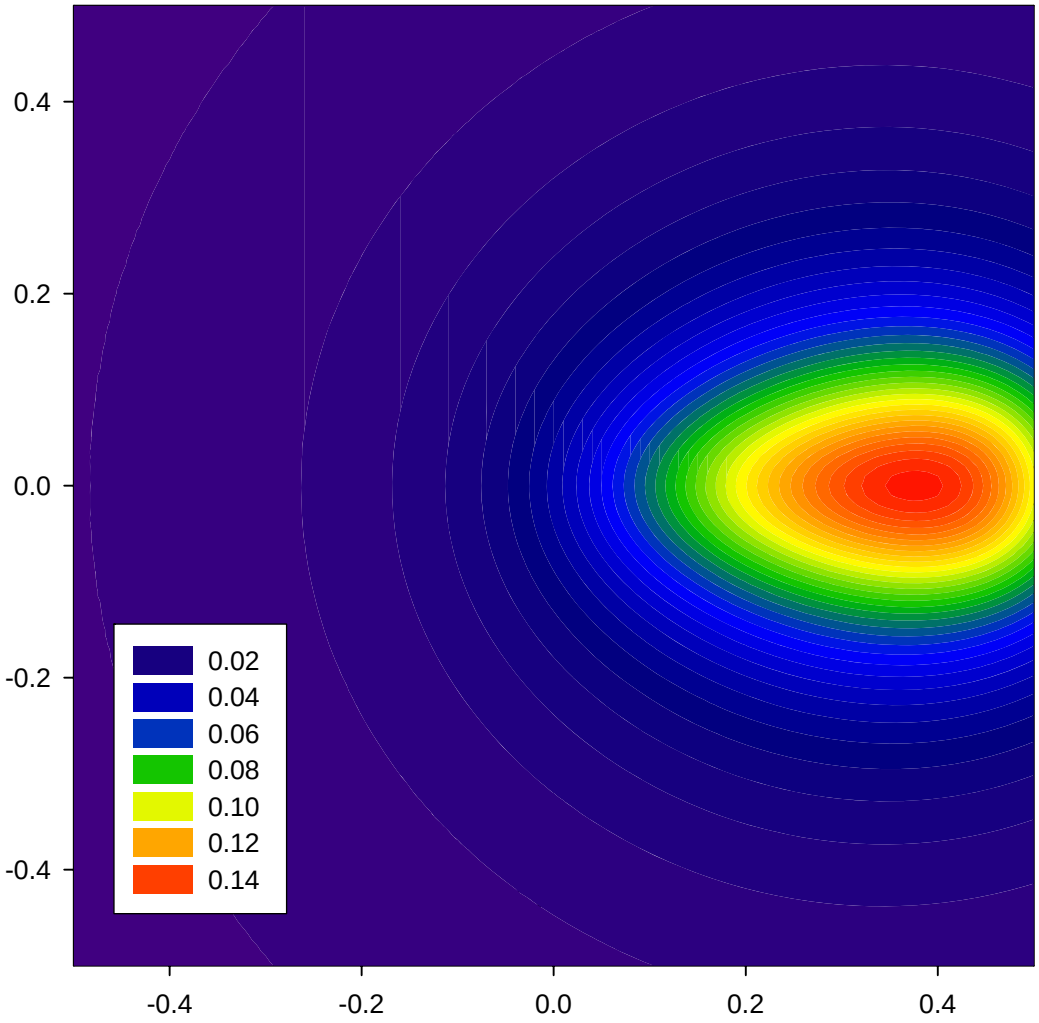

Fig. 4a 15 Deg partial disk source viewed 0.1 mfp from source

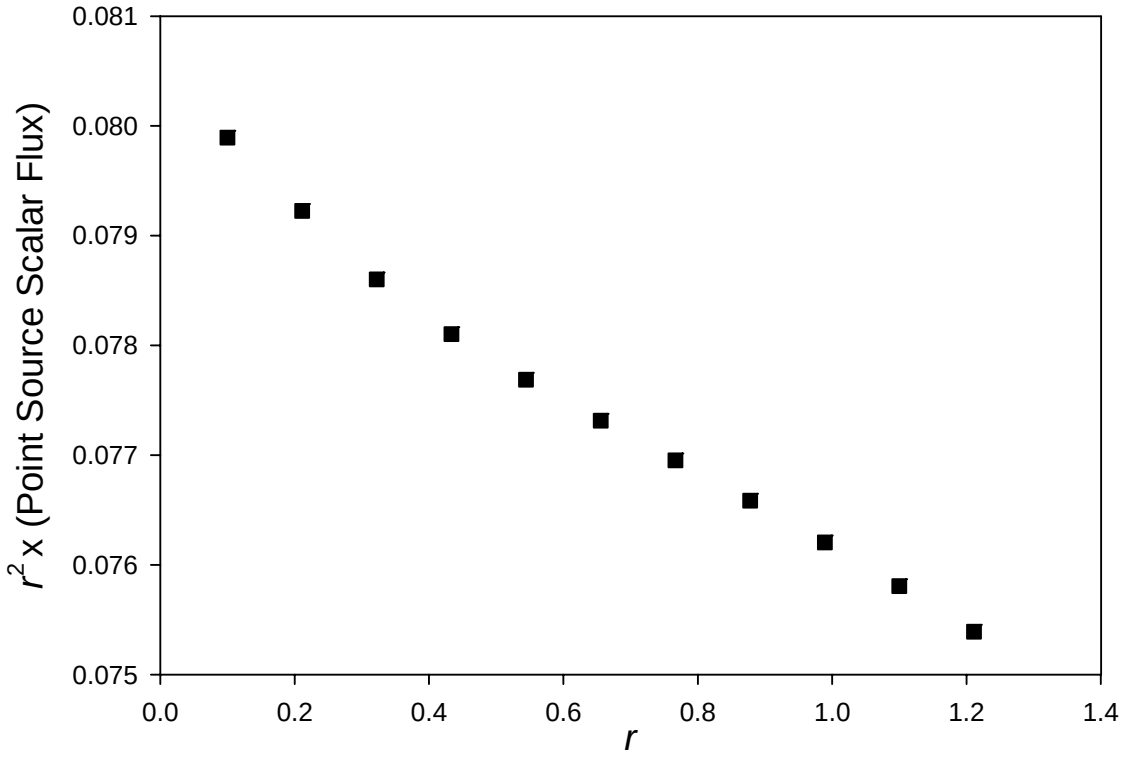

Fig. 4b $r^2\phi_{pt}(r)$ for N_{int} = 10 in the interval $[r_{min}, r_{max}]$

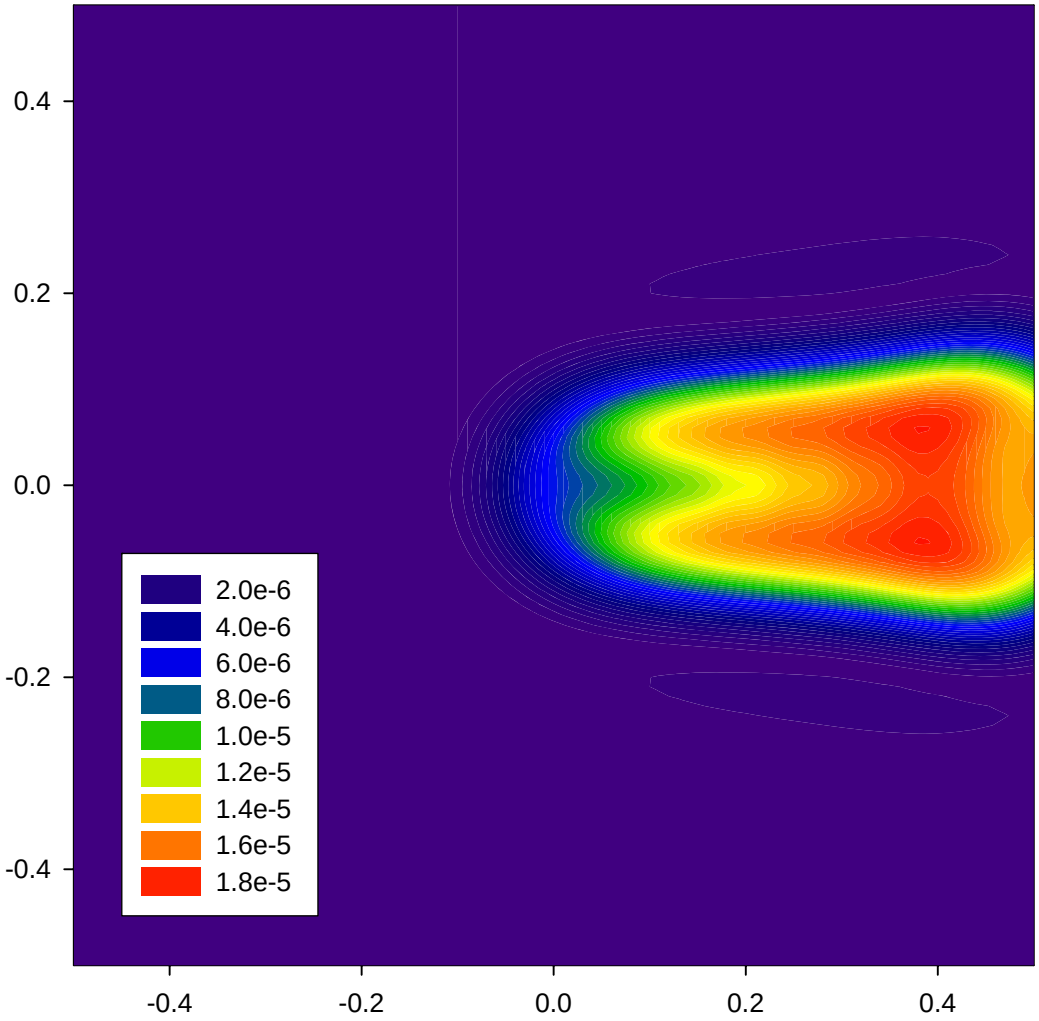

Fig. 4c Relative error of N_{int}=10 interpolation to full evaluation.

Table 1--Convergence in Quadrature Order

Lm	*Relative Error*
2	----------
4	3.82E-01
6	6.81E-02
8	1.30E-02
10	2.62E-03
12	5.28E-04
14	1.10E-04
16	2.22E-05

Table 2 Comparison of **EVENT** with the Point Source Benchmark

		1D spherical geometry (200 linear elements)			*3D geometry (400,000 linear tetrahedral elements and 90000 nodes)*		
Radius	*Reference Flux*	P_1	P_7	P_{11}	P_1	P_7	P_{11}
1.05930E+00	1.29113E-01	1.26423E-01	1.28764E-01	1.28596E-01	1.30293E-01	1.36115E-01	1.34021E-01
2.03365E+00	3.58033E-02	3.85618E-02	3.57483E-02	3.57957E-02	3.99724E-02	3.53938E-02	3.55217E-02
3.00800E+00	1.40411E-02	1.52743E-02	1.40269E-02	1.40182E-02	1.55817E-02	1.39081E-02	1.39425E-02
4.05730E+00	5.92296E-03	6.37744E-03	5.91907E-03	5.91615E-03	6.52853E-03	5.88889E-03	5.88386E-03
5.03165E+00	2.84871E-03	3.03727E-03	2.86742E-03	2.86501E-03	3.08451E-03	2.78993E-03	2.79001E-03
6.00600E+00	1.42717E-03	1.48056E-03	1.42362E-03	1.42437E-03	1.51347E-03	1.38210E-03	1.38212E-03
7.05530E+00	6.99215E-04	7.09703E-04	6.96974E-04	6.98249E-04	7.25802E-04	6.74254E-04	6.74044E-04
8.02965E+00	3.68015E-04	3.65633E-04	3.67041E-04	3.67304E-04	3.71343E-04	3.50791E-04	3.50562E-04
9.00400E+00	1.96640E-04	1.91133E-04	1.96385E-04	1.96093E-04	1.95625E-04	1.87856E-04	1.87708E-04
1.00533E+01	1.01459E-04	9.93875E-05	1.04584E-04	1.04275E-04	1.00835E-04	9.87455E-05	9.86739E-05
1.10276E+01	5.54300E-05	5.15240E-05	5.55030E-05	5.53390E-05	5.22985E-05	5.21816E-05	5.21615E-05
1.20020E+01	3.05224E-05	2.77488E-05	3.05344E-05	3.04761E-05	2.81973E-05	2.85644E-05	2.85545E-05
1.30513E+01	1.61721E-05	1.43663E-05	1.61576E-05	1.61524E-05	1.45929E-05	1.51222E-05	1.51056E-05
1.40257E+01	9.01891E-06	7.83473E-06	8.98748E-06	8.99726E-06	7.90660E-06	8.38815E-06	8.37197E-06
1.50000E+01	5.05411E-06	4.28916E-06	5.01767E-06	5.02869E-06	4.35838E-06	4.70787E-06	4.70047E-06